

Chapter 7

Research Article 3: Synthesis, Evaluation and Application of Polycyclic Fluorescent Analogues as NMDA Receptor and VGCC Ligands

Article published online on 11 August 2011

European Journal of Medicinal Chemistry 46 (2011) 5010-5020

Synthesis, Evaluation and Application of Polycyclic Fluorescent Analogues as N-Methyl-D-Aspartate Receptor and Voltage Gated Calcium Channel Ligands

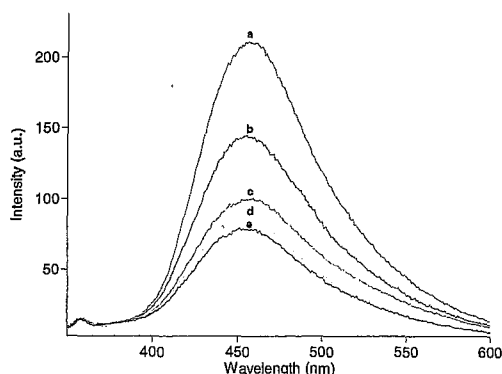
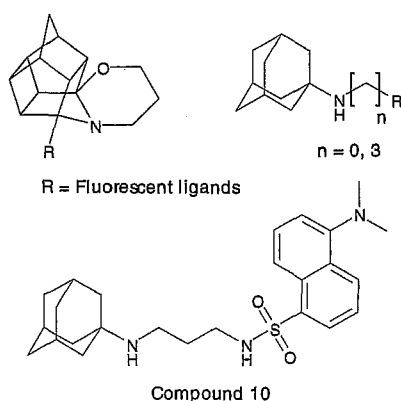
Jacques Joubert^{a,b} Sandra v Dyk^a Ivan R. Green^c and Sarel F. Malan^{a,b,*}

^aPharmaceutical Chemistry, North-West University, Private Bag 6001, Potchefstroom, 2520, South Africa.

^bSchool of Pharmacy and ^cDepartment of Chemistry, University of the Western Cape, Bellville, South Africa, Private Bag X17, Bellville 7535, South Africa.

*Corresponding author at present address: School of Pharmacy, University of the Western Cape, Private Bag X17, Bellville 7535, South Africa. Tel: +27 21959 3190; fax: +27 21959 1588; e-mail: sfmalan@uwc.ac.za

Graphical abstract



Article Highlights

- Fourteen polycyclic fluorescent compounds were synthesized and evaluated for inhibition of calcium flux *via* the *N*-methyl-D-aspartate receptor (NMDAR) and voltage gated calcium channel (VGCC).
- Compounds **3**, **5**, **7**, **8**, **9**, **10** and **14** displayed significant NMDAR antagonistic activity with compounds **7**, **8**, **10** and **11** exhibiting significant VGCC inhibition.
- The IC₅₀ value of compound **10** was calculated at 0.27 μ M with a maximum inhibition of 37.41% at a concentration of 100 μ M showing potent NMDAR inhibition comparable to MK-801 at the same concentration.
- Compound **10** was further used as a fluorescent NMDAR ligand in a fluorescent competition assay utilizing known NMDAR inhibitors to demonstrate the possible applications of these novel fluorescent analogues.

Abstract

A series of polycyclic fluorescent ligands were synthesised and evaluated in murine striatal synaptoneuroosomes for *N*-methyl-D-aspartate receptor (NMDAR) mediated calcium flux inhibition and inhibition of calcium influx through voltage gated calcium channels (VGCC). Amantadine (**a**) and *N*-(1-adamantyl)-1,3-propanediamine (**c**) substituted with 1-cyanoisindole (**3**), indazole (**5**), dinitrobenzene (**7**, **8**), dansyl (**9**, **10**) and coumarin (**11**) moieties showed moderate to high inhibition of the NMDAR. A high degree of VGCC inhibition was observed for the cyanoisindole compounds (**3**, **4**) the dansyl compounds (**9**, **10**) and the coumarin compound (**12**). Fluorophores conjugated to hydroxy-4-aza-8-oxoheptacyclotetradecane (**13**, **14**) did not exhibit any significant VGCC inhibition, but the indazole conjugate (**14**) showed promising NMDAR activity. Dose response curves were calculated for selected NMDAR inhibitors (**8** - **11**) and *N*-[3-(1-adamantylamino)propyl]-5-dimethylaminonaphthalene-1-sulfonamide (**10**) exhibited the highest activity of the novel compounds. Compound **10** was further used as a fluorescent NMDAR ligand in a fluorescent competition assay utilizing MK-801, NGP1-01 and amantadine as known NMDAR inhibitors to demonstrate the possible applications of the novel fluorescent compounds. These small molecule fluorescent ligands can be considered as

possible pharmacological tools in assay development and/or other investigations in the study of neurodegeneration.

Keywords: Polycyclic, Amantadine, NMDAR, Calcium Channels, Fluorescent Ligands.

7.1. Introduction

Neurodegeneration and the development of neuroprotective agents have in recent years become an increasingly important focus of research. Much time and effort have gone into establishing the cause and markers of disorders like Parkinson's disease (PD) and Alzheimer's disease (AD) as they negatively influence the quality of life of millions of people around the world [1]. Neurodegeneration can be described as the process by which certain neurons in the central nervous system (CNS), and especially the brain, are damaged by a variety of mechanisms [2]. These disorders are characterized by progressive and irreversible loss of neurons from specific regions of the brain [3]. Amongst the mechanisms implicated to be responsible for neuronal cell death, we have focused our interest on excitotoxicity.

The *N*-methyl-D-aspartate receptor (NMDAR) has been suggested as a drug target through its involvement in neurodegenerative disorders such as PD and AD [4]. Overstimulation of the NMDAR by an excess of the endogenous neurotransmitter glutamate during pathological conditions leads to excessive influx of extracellular calcium into neuronal cells resulting in cell death, a process known as excitotoxicity [5]. Calcium entry through voltage gated calcium channels (VGCC) also contributes to calcium overload and mitochondrial disruption that leads to the recruitment or release of mediators responsible for the activation of an apoptotic cascade and ultimately, in cell death [4]. Several authors have described the link between glutamate toxicity and calcium influx through the NMDAR and VGCC [4-7]. The subsequent calcium overload and observed excitotoxicity lead to the idea that glutamate toxicity participated in neuronal cell death [6]. This link also established a specific rationale for targeting the NMDAR and/or VGCC for selective blockade of extraneous calcium fluxes, thus allowing subsequent reduction in glutamate-induced calcium influx [7].

Several polycyclic compounds (Figure 1) have been identified as NMDAR antagonists. This includes the high-affinity noncompetitive NMDAR antagonists (MK-801 and PCP) and low affinity uncompetitive NMDAR antagonists (amantadine, memantine and NGP1-01) [8]. MK-801 and PCP bind to the PCP binding site located within the ion-channel pore of the NMDAR [9]. This antagonism is use dependent in that the PCP site is only accessible when

the ion channel pore is in an open, or activated state [9]. The block is enhanced by increases in open channel probability. This phenomenon implies that compounds with pronounced use-dependency will have greater affinity for the brain region where overstimulation occurs [10]. Once bound, the blocker can be trapped by channel closure. Amantadine, memantine and NGP1-01 modulate the NMDAR channel, rather than blocking it completely as is the case for the high-affinity noncompetitive NMDAR antagonists [6,9]. Thus, the low-affinity uncompetitive NMDAR channel antagonists only modulate the NMDAR channel during excessive calcium flux and remain in the channel long enough to reduce excessive calcium influx, operating in a use dependent manner that allows for normal neuronal functioning [9]. Because of this low affinity, amantadine and NGP1-01 is speculated to leave the receptor site before the channel closes [8-10]. NGP1-01 is described as having a dual mechanism of action by blocking both the NMDAR and *L*-type calcium channels, with its neuroprotective activity confirmed by *in vivo* studies [11-16].

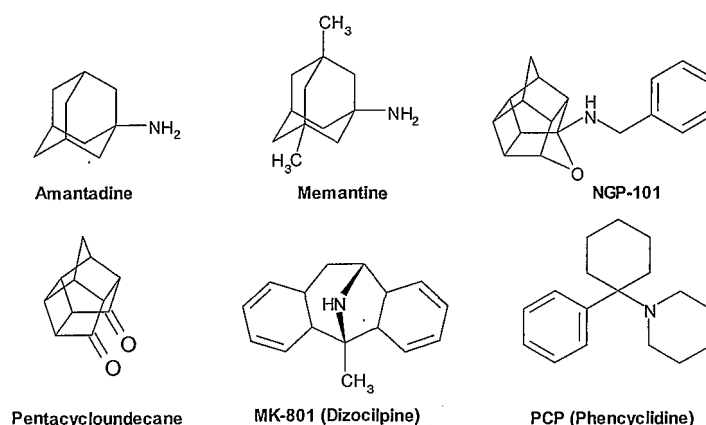


Figure 1: Representative polycyclic structures as NMDAR and/or calcium channel modulators [8,9].

Radioligand binding techniques have been widely used to study receptor pharmacology and physiology [17]. Geldenhuys *et al.* described the characterisation of polycyclic compounds derived from the pentacycloundecane structure and their interaction with NMDAR by means of radioligand binding studies [8]. Despite the usefulness and sensitivity of radioligand binding techniques, the use of alternative methods (for instance fluorescent techniques) to study receptor-ligand binding interactions may provide information not readily accessible by conventional radioreceptor techniques and circumvent some of the drawbacks, such as high cost, disposal, health hazard and potential technical implications, associated with this methodology [18]. Techniques to visualize physiological or pathophysiological changes in living cells have become increasingly important in biomedical sciences. Fluorescent probes

are excellent tools to analyze and clarify the roles of biomolecules in living cells, affording high spatial and temporal resolution *via* microscopic imaging. The development of tools for probing biological events has thus become an area of intense interest [19,20].

We report here the results of our efforts to design a polycyclic fluorescent ligand for the NMDAR and possibly VGCC with the aim of enabling development of fluorometric assays to assist in the quest for effective neuroprotective strategies. Fluorometric assays offer several advantages over their radiometric counterparts *viz*; to determine properties like receptor internalization and sub cellular localization, the thermodynamics and kinetics of ligand binding and to assess the nature of the microenvironment of the ligand binding site [21]. The greatest challenge in the design of fluorometric assays lies in the development of a fluorescent ligand while maintaining potency and accommodating steric demands of the fluorophore, especially when the fluorescent moiety is conjugated to a small molecule. Nonetheless, there have been several reports of successful fluorophore-conjugation with small molecule ligands [22,23], and recent advances in fluorometric assays utilising fluorescent ligands [22] has encouraged pursuit of this approach.

In our efforts to design a fluorescent polycyclic NMDAR and/or calcium ligand we utilized the amantadine and 3-hydroxy-4-aza-8-oxoheptacyclotetradecane polycyclic moieties as the NMDAR and/or calcium channel inhibitors conjugated to various fluorescent ligands. The adamantane and polycyclic moieties were selected because of their known affinity for VGCC and uncompetitive NMDAR channel antagonism which modulates rather than blocks the NMDAR channel completely and allows normal neuronal functioning [6,9]. It is hypothesized that these polycyclic moieties will be effective scaffolds to conjugate to small molecule fluorescent compounds and to use these molecules to gain a better understanding of the mechanism of action involved in modulation of NMDAR and/or calcium channel activity utilizing fluorescent high-throughput assays.

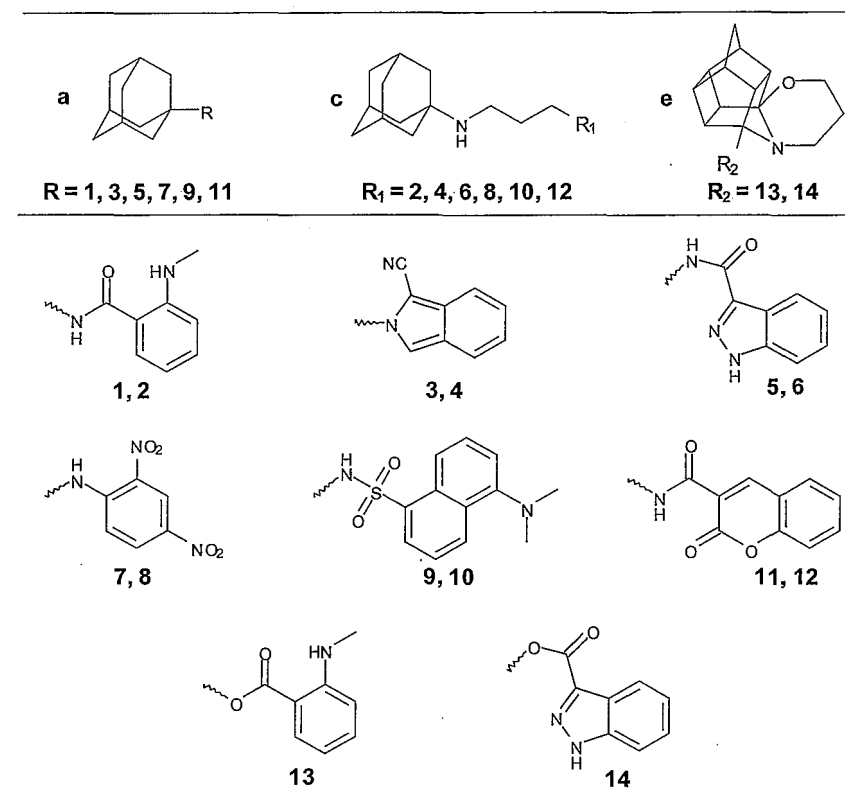
7.2. Chemistry

The fluorescent ligands for this study were selected on the basis of their spectroscopic properties and structural requirements for VGCC and NMDAR inhibition. These ligands were successfully conjugated to amantadine (**a**) and 3-hydroxy-4-aza-8-oxoheptacyclotetradecane (**e**) by means of direct conjugation employing methods previously described [24,25]. 3-Hydroxy-4-aza-8-oxoheptacyclotetradecane (**e**) was synthesized by reacting

7.3. Pharmacology

NMDAR and VGCC activity of the test compounds were evaluated on murine synaptoneurosomes utilizing the fluorescent ratiometric calcium indicator, Mag-Fura-2/AM, and a Cary Eclipse[®] fluorescence spectrometer system [29]. All novel fluorescent compounds and controls were tested at 100 μ M, to identify active VGCC and/or NMDAR calcium influx inhibitors. NMDAR dose response curves were calculated for selected compounds which showed a high degree of NMDAR inhibition. From these studies *N*-[3-(1-adamantylamino)propyl]-5-dimethylaminonaphthalene-1-sulfonamide (**10**) was identified as a potent NMDAR inhibitor. Compound **10** was further utilized as a fluorescent NMDAR ligand in a competition assay where we utilized different polycyclic NMDAR inhibitors to compete with compound **10** for binding of the NMDAR and demonstrate the possible application(s) of these novel fluorescent ligands.

Table 1: Fluorescent derivatives conjugated to amantadine (**a**), *N*-(1-adamantyl)-1,3-propanediamine (**c**) and 3-hydroxy-4-aza-8-oxoheptacyclotetradecane (**e**)



3-aminopropanol with the well described Cooksen diketone (**d**) [26,27] with subsequent intramolecular cyclisation and dehydration to form **e** [28]. To reduce structural hindrances and achieve potentially greater affinity for the VGCC and the NMDAR, we also synthesised an adamantane molecule with a 3-carbon spacer [*N*-(1-adamantyl)-1,3-propanediamine] separating the conjugated fluorophore and the amantadine moiety. *N*-(1-Adamantyl)-1,3-propanediamine (**c**) was synthesized by Michael addition utilizing acrylonitrile to give 3-(1-adamantylamino)propionitrile (**b**) and subsequent reduction of the nitrile with LiAlH to form the desired primary amine (**c**, Figure 2).

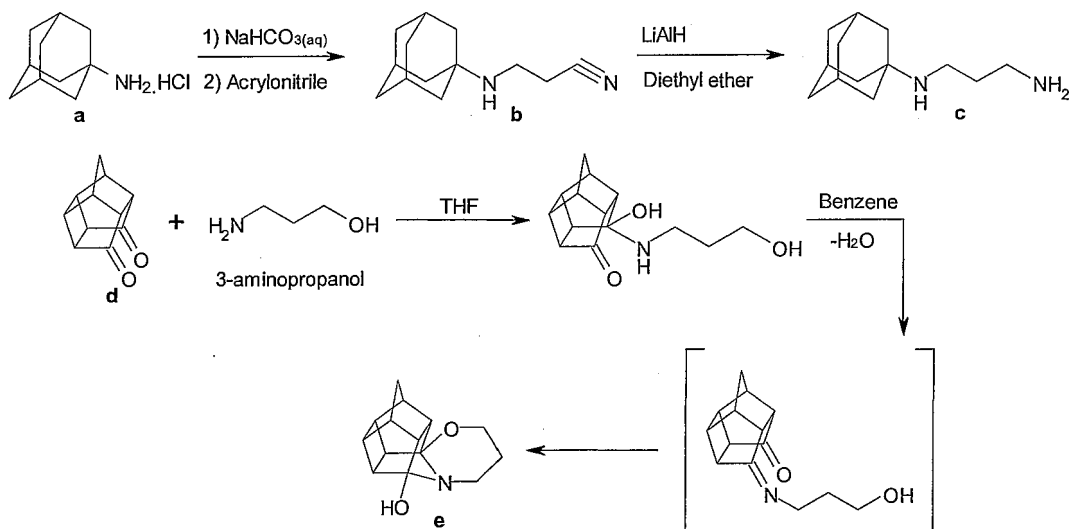


Figure 2: General reaction schemes for the synthesis of *N*-(1-adamantyl)-1,3-propanediamine (**c**) and 3-hydroxy-4-aza-8-oxoheptacyclotetradecane (**e**)

The fluorescent molecules utilized for evaluation of VGCC and NMDAR activity included: *N*-methylantranilic acid, indazole-3-carboxylic acid, 1-fluoro-2,4-dinitrobenzene, 1-cyanoisindole, dansyl chloride and coumarin-3-carboxylic acid. These compounds were conjugated to amantadine, *N*-(1-adamantyl)-1,3-propanediamine and 3-hydroxy-4-aza-8-oxoheptacyclotetradecane by various synthetic methods including activation chemistry, amination, amidation and esterification. The synthesised compounds (Table 1) were all obtained as oils or amorphous solids from chromatography or were crystallized from organic solvents. Structures were confirmed using ¹H and ¹³C NMR, IR and MS.

7.4. Results and discussion

7.4.1. VGCC calcium influx inhibition

The amantadine and 3-hydroxy-4-aza-8-oxoheptacyclotetradecane fluorescent compounds were evaluated for VGCC activity because of their structural similarities towards the calcium channel inhibitor NGP1-01. In the ratiometric imaging experiments using Mag-fura-2AM as fluorescent calcium indicator, application of high concentration potassium (140 mM) resulted in an increase in the fluorescent ratio in the presence of extracellular calcium. This increase in fluorescence indicates an influx of calcium through VGCC. The reference compounds nimodipine, a commercially available dihydropyridine *L*-type calcium channel blocker, NGP1-01 and amantadine exhibited statistically significant average decreases in fluorescence, and subsequent decrease in calcium influx, 87.71%, 29.88% and 13.87% respectively, when compared to the KCl control treated synaptoneurosomes (Figure 3). Synaptoneurosomes incubated with test compounds **3**, **4**, **9**, **10** and **12** showed the most significant inhibition of calcium influx with decreases in fluorescence of 45.76%, 54.08%, 55.23%, 63.26% and 32.01%, respectively. All these compounds demonstrated significantly better inhibition ($p < 0.05$) than the reference polycyclic compounds NGP1-01 and amantadine (Figure 3 and Table 2), with compound **10** exhibiting the highest activity (63.26%). Compounds **11**, **13** and **14** also had notable decreases ($p < 0.05$) in fluorescence of 24.65%, 15.21% and 16.38%. Test derivatives **1**, **2**, **5**, **6**, **7** and **8** had weak VGCC activity.

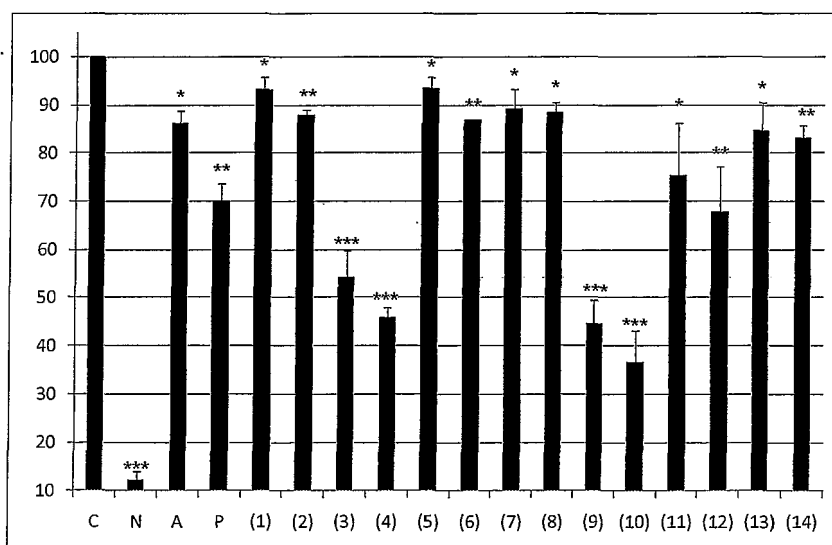


Figure 3: Screening of test compounds (100 μ M, $n = 9$) for antagonism of KCl-mediated calcium influx *via* VGCC into murine striatal synaptoneurosomes. Each bar represents mean percentage of control values \pm SEM. Abbreviations are: control (C), nimodipine (N), NGP1-01 (P) and amantadine (A). Statistical analysis (ANOVA) was performed on raw data, with asterisks signifying significant inhibitory effect [(*) $p < 0.05$, (**) $p < 0.01$ and (***) $p < 0.001$] when compared to the control (100%).

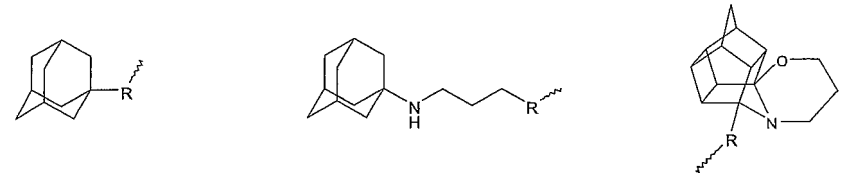
We found that the increase in chain length between the amantadine moiety and the fluorophores generally lead to a increase in calcium channel blocking activity, whereas direct attachment of the fluorophores to amantadine noticeably reduced the activity for calcium channel blockage. For the cyanoisindole compounds (**3** and **4**) and the dansyl compounds (**9** and **10**) an increase in chain length led to a significant ($p < 0.05$) increase in activity (Figure 3 and Table 2). The same tendency (though not significant; $p > 0.05$) was observed for the anthranilic (**1**, **2**), indazole (**5**, **6**), and the coumarin (**11**, **12**) derivatives. This correlated with the study by Liebenberg *et al.* which found that an increase in chain length between the polycyclic and aromatic moieties led to an increase in calcium channel antagonistic activity [30]. It can be argued that an increase in chain length might indicate that a deeper immersion into the calcium channel may be obtained for stronger interaction with the putative binding site. The tetradecane fluorescent moieties (**13**, **14**) have low calcium channel activity, only slightly better than amantadine. The compounds with significant VGCC activity (Table 2) all contain bicyclic aromatic functionalities (**3**, **4**, **9**, **10** and **11**) in their structures, showing a significant increased degree of VGCC inhibition when compared to their monoaromatic counterparts (**1**, **2**, **7**, **8** and **13**). The isindole (**3**, **4**), dansyl (**9**, **10**) and coumarin (**11**) functional moieties contained in these structures are described throughout literature as privileged structures. Further development of these structures however needs to be conducted to elaborate on their true potential as VGCC inhibitors and to develop structure activity relationships for this series of fluorescent compounds (Figure 3 and Table 2).

Compounds **9** and **10**, with high affinity for the voltage gated calcium channels, has long wavelength fluorescence (334/517 and 324/455, respectively), high stokes shifts (183 and 131, respectively) and strong affinity for calcium channels (Table 2). Compounds **3** and **4** also show promise as possible fluorescent ligands for the calcium channel but have short fluorescent wavelengths (358/395 and 360/400, respectively) and low Stokes shifts (37 and 40, respectively), which could be unfavorable in some fluorescent imaging techniques. Compounds **9** and **10** could thus be utilized as potential fluorescent ligands for imaging of calcium channels using modern fluorescent imaging techniques.

Intermediates **b**, **c** and **e** were also screened for calcium channel activity and interesting findings were observed. *N*-(1-Adamantyl)-1,3-propanediamine (**c**) and 3-Hydroxy-4-aza-8-oxoheptacyclotetradecane (**d**) showed modest calcium channel inhibitory activity, weaker than all reference test compounds (Table 2). Importantly, intermediate

3-(1-adamantylamino)propionitrile (**b**) exhibited a high degree of calcium influx inhibition (36.72% decrease in fluorescence) superior to NGP1-01 and amantadine. This could indicate that the nitrile group was involved in favorable binding interactions with calcium channels and reduction thereof to the secondary amine (compound **c**) drastically decreased activity. Both compounds **3** and **4** contain nitrile groups and exhibited high calcium channel blocking activity. These important findings may lead to further development of compounds derived from nitrile containing leads to develop potent calcium channel inhibitors.

Table 2: Summary of effects the polycyclic fluorescent derivatives and related compounds on KCl induced calcium influx inhibition (at 100 μ M), inhibition of NMDA/glycine (N/G) induced calcium influx (at 100 μ M) and fluorescent properties of the compounds.



Compound	R (Fluorophore)	Compounds 1, 3, 5, 7, 9, 11		Compounds 2, 4, 6, 8, 10, 12		Compounds 13, 14	
		% Ca ²⁺ -flux after KCl stimulation ^{a,*}	% Ca ²⁺ -flux after N/G stimulation ^{a,*}	cLog P	λ_{ex} (nm) ^b	λ_{em} (nm) ^b	
1	<i>N</i> -Methylantranilamido	93.20 \pm 2.69*	96.66 \pm 4.89	4.24 \pm 0.40	366	415	
2	<i>N</i> -Methylantranilamido	87.91 \pm 1.12**	88.02 \pm 4.25	4.12 \pm 0.42	360	420	
3	1-Cyanoisoindole	54.24 \pm 5.45***	84.01 \pm 5.53*	4.88 \pm 0.35	358	395	
4	1-Cyanoisoindole	45.92 \pm 2.03***	86.41 \pm 4.12	3.32 \pm 0.42	360	400	
5	1 <i>H</i> -Indazole-3 carboxamido	93.43 \pm 2.34*	83.70 \pm 0.99*	3.02 \pm 0.43	340	400	
6	1 <i>H</i> -Indazole-3 carboxamido	86.91 \pm 0.11*	95.19 \pm 6.67	3.14 \pm 0.40	340	405	
7	2,4-Dinitrophenyl-1-amine	89.14 \pm 4.10*	80.75 \pm 6.27*	5.54 \pm 0.32	396	449	
8	2,4-Dinitrophenyl-1-amine	88.50 \pm 2.09*	76.59 \pm 9.55*	5.13 \pm 0.35	390	430	
9	Dansylamido	44.77 \pm 4.70***	78.05 \pm 5.41*	5.54 \pm 0.38	334	517	
10	Dansylamido	36.74 \pm 6.47***	62.97 \pm 8.21*	5.42 \pm 0.40	324	455	
11	Coumarin-3-carboxamido	75.35 \pm 11.0*	79.71 \pm 4.42*	3.53 \pm 0.75	364	407	
12	Coumarin-3-carboxamido	67.99 \pm 9.37**	86.77 \pm 5.71	3.41 \pm 0.75	360	410	
13	2-Methylaminobenzoate	84.79 \pm 5.76*	86.41 \pm 4.11	2.63 \pm 0.72	366	415	
14	1 <i>H</i> -Indazole-3-carboxylate	83.62 \pm 2.54**	77.89 \pm 8.23*	1.53 \pm 0.72	330	410	
Nimodipine	-	12.29 \pm 1.66***	n.d.	3.85 \pm 0.59	-	-	
Amantadine	-	86.13 \pm 3.63*	83.10 \pm 2.98*	2.22 \pm 0.24	-	-	
MK-801	-	n.d.	64.04 \pm 2.62**	3.68 \pm 0.39	-	-	
NGP1-01	-	70.12 \pm 2.69***	86.63 \pm 1.03**	1.68 \pm 0.36	-	-	
c	-	63.28 \pm 4.26***	80.71 \pm 1.44**	2.10 \pm 0.28	-	-	
d	-	89.33 \pm 3.54*	90.99 \pm 6.20	2.10 \pm 0.26	-	-	
e	-	87.24 \pm 2.14*	77.29 \pm 2.11*	0.33 \pm 0.60	-	-	

^aControl was taken as 100% calcium influx. Asterisks signifying statistical significance, (*) $p < 0.05$, (**) $p < 0.001$ and (***) $p < 0.0001$. ^a% Control \pm SEM ($n = 3$); ^bAt 10^{-5} M in DMSO at 25 $^{\circ}$ C; λ_{ex} = excitation λ ; λ_{em} = emission λ ; n.d. = not determined.

7.4.2. NMDAR calcium influx inhibition

The effects of the novel polycyclic fluorescent moieties of representative experiments in the presence and absence of test compounds and reference compounds (100 μ M) on NMDA/glycine-mediated calcium influx into synaptoneurosomes are shown in Table 2 and

Figure 4. Incubation with the reference compounds MK-801, NGP1-01 and amantadine showed statistically significant average decreases in fluorescence of 35.96%, 13.37% and 16.9% respectively, when compared to the NMDA/glycine control synaptoneurosomes. A statistically significant ($p < 0.05$) decrease in fluorescence was also observed for compounds **3**, **5**, **7**, **8**, **9**, **10**, **11** and **14** (16% - 39%) when compared to the control. All of these fluorescent molecules showed enhanced inhibition compared to that of the references, NGP1-01 and amantadine (Figure 4 and Table 2), with compound **10** (37.03%) exhibiting the highest inhibition of NMDAR calcium influx of the novel inhibitors, comparable to MK-801 (35.96%). Compounds **2**, **4**, **12** and **13** exhibited slight, though not statistically significant NMDAR inhibition between 11.98% and 13.59%. Compounds **1** and **6** showed no discernable NMDAR inhibitory activity. Dose-response curves were constructed (Figure 5) for selected active NMDAR inhibitors (**8** - **11**). The solubility of these novel compounds however became a limiting factor at higher concentrations and compounds were only tested to a maximum concentration of 100 μM before precipitation occurred. From this data it was clear that compound **10** had the highest activity at all concentrations (Figure 5) with an IC_{50} value of 0.27 μM and maximum inhibition of 37.41% at a concentration of 100 μM .

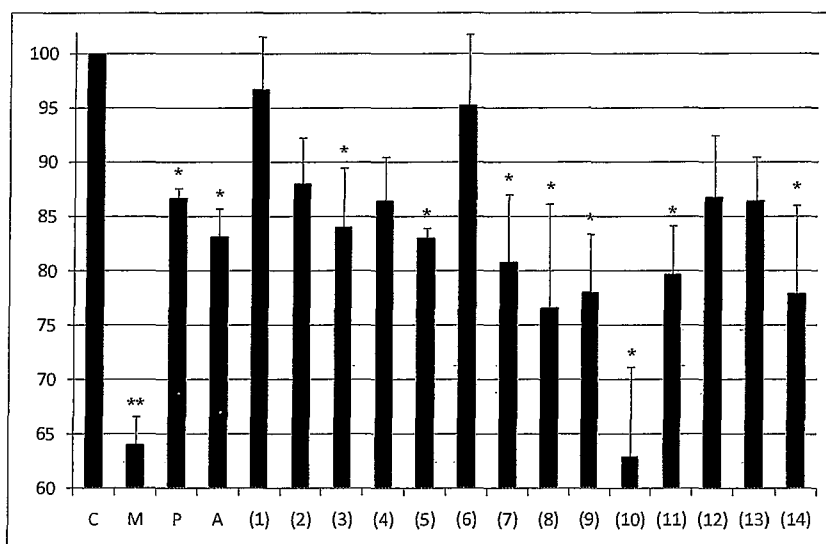


Figure 4: Screening of test compounds (100 μM , $n = 9$) for antagonism NMDAR-mediated calcium influx into murine striatal synaptoneurosomes. Each bar represents mean percentage of control values \pm SEM. Abbreviations are: Control (C), MK-801 (M), NGP1-01 (P) and amantadine (A). Statistical analysis was performed on raw data, with asterisks signifying significant inhibitory effect [(*) $p < 0.05$, (**) $p < 0.001$] when compared to the control (100%).

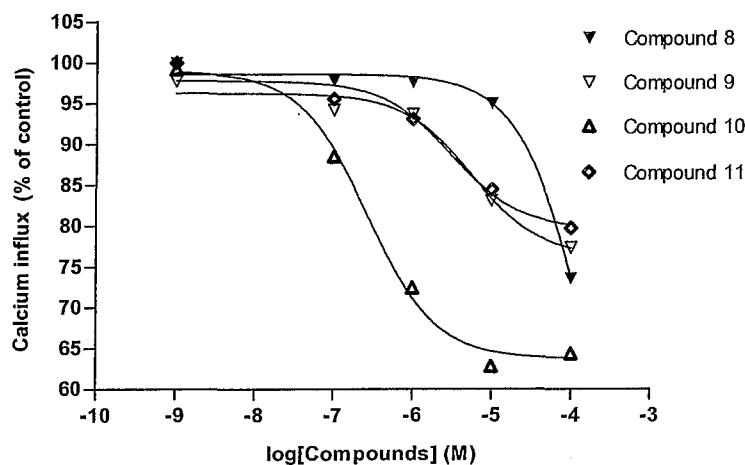


Figure 5: Inhibition curves of compounds 8 - 11 with meaningful NMDAR activity were superimposed to compare their potencies at different concentrations.

According to previous studies [8,31], an increase in affinity for the NMDAR channel may be associated with an increase in hydrophobicity. Log *P* values were calculated (ACD Labs/Chemsketch[®]) for the test compounds and were found to be higher than that of the reference compounds (Table 2). The highest Log *P* values were predicted for compounds 7, 8, 9, and 10 (Log *P* > 5), some of the most potent inhibitors amongst the novel inhibitors. The inhibition observed for these derivatives correlates to the high lipophilicity, with subsequent high permeability across biological membranes, and favorable steric interactions of the fluorophores with the NMDAR. In our study the compounds with a greater molecular size, to a certain degree, lead to an increase in activity. This could however also be attributed to the high lipophilicity of the novel compounds and interactions of the fluorophores with certain residues in the receptor binding pocket (Table 2 and Figure 4). The increase in the chain length of the adamantyl fluorophores in general gave more favourable steric and electronic interactions between the fluorophores and the residues in the receptor binding pocket, than the more sterically hindered directly conjugated moieties.

The compounds with biaromatic functionalities in their structures in general showed better NMDAR antagonistic activity, with the dinitrobenzene derivatives also having significant NMDAR activity (Table 2). The activity of the dinitrobenzene compounds could probably be ascribed to additional interactions or inclusion of other mechanisms of action for these derivatives in the NMDAR channel. One hypothesis is that the nitro functionalities could contribute to the S-nitrosylation of cysteine residues in the NMDAR channels, thus increasing NMDAR inhibitory activity [32, 33]. Further development of the high affinity NMDAR

inhibitors identified in this study will elaborate on structure activity relationships of these compounds.

Intermediates **b**, **c** and **e** were also screened for NMDAR activity with 3-(1-adamantylamino)propionitrile (**b**) and 3-hydroxy-4-aza-8-oxoheptacyclotetradecane (**e**) showing significant (19.29% and 22.71%, respectively) NMDAR inhibition (Table 2). 3-(1-Adamantylamino)propionitrile (**b**) exhibited better activity than its primary amine counterpart *N*-(1-adamantyl)-1,3-propanediamine (**c**, 9.01%). This could indicate that the nitrile group is involved in favorable binding interactions with the NMDAR. 3-Hydroxy-4-aza-8-oxoheptacyclotetradecane exhibited good inhibitory activity (22.71%) compared to the reference compounds and substitution thereof with the 1*H*-indazole-3-carboxylate moiety (**13**) retained activity (22.11%), whereas the 2-methylaminobenzoate (**14**) substitution decreased activity (13.59%).

7.4.3. NMDAR competition assay utilizing *N*-[3-(1-adamantylamino)propyl]-5-dimethylamino-naphthalene-1-sulfonamide (**10**)

A competition assay was developed as proof of concept for the potential use of these novel fluorescent polycyclic compounds in biological applications. It could also confirm the binding site of compound **10** when compared to known NMDAR antagonists. Compound **10** was used as a fluorescent ligand for these assays, due to its relatively potent antagonism of NMDAR-stimulated calcium influx into murine synaptoneurosomes (Table 2), long fluorescent wavelength (324_{Ex}/455_{Em}) and high stokes shift (131 nm). Both amantadine and MK-801 binds to the PCP binding site deep within the NMDAR channel [9,34]. The synthesised adamantane fluorophores share the same polycyclic amine template and we postulated that these compounds should also interact with the PCP binding site within the ion channel of the NMDAR.

Results of the novel competition binding assay are depicted in figures 6 and 7. MK-801 decreased the fluorescent intensity of the experimental sample by 46.03%, indicating the equipotence of the two molecules (Figures 6 and 7). The displacement of **10** by amantadine (36.30%) further confirms the binding of this fluorophore at the PCP site. NGP1-01 have been reported to have no binding affinity for the PCP binding site but to interact with a unique binding site, different to that reported for MK-801 or PCP, in the NMDA receptor/ion channel complex [8,12]. In our study NGP1-01 also competed for binding with compound **10** (17%),

but to a lesser extent to that of amantadine and MK-801. This suggests that compound **10** probably interacts with a further binding site, other than the PCP binding site. One hypothesis for the decrease in fluorescent intensity of compound **10** by NGP1-01 would be to suggest that the dansyl moiety undergoes aromatic interaction with (an) aromatic amino acid(s) located at the entrance of the NMDA receptor channel- the site where NGP1-01 interacts [12]. Such an interaction would allow the molecule to be 'anchored' in such a way that the adamantine moiety can descend into the channel lumen to a depth allowed by the linker between amantadine and the dansyl moiety. In support of this hypothesis, the ability of MK-801 and amantadine to compete with compound **10** for the PCP binding site may be a result of its longer linkage, allowing the amantadine moiety to explore deeper into the channel to reach the proximity of the PCP binding site. This is probably the reason why the compounds incorporating the linker in general (**7**, **8**, **9** and **10**, Table 2) showed better inhibition of the NMDAR.

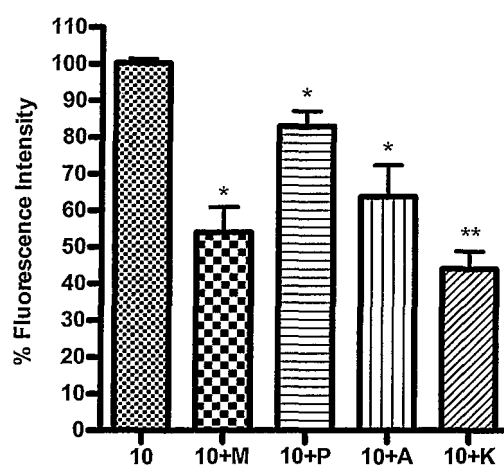


Figure 6: Fluorescent intensities of NMDA/glycine-mediated competition assay utilizing compound **10** (100 μ M) and known NMDAR inhibitors. Each bar represents mean percentage values \pm SEM ($n = 9$). Abbreviations are: MK-801 (M), NGP1-01 (P), Amantadine (A) and (K) a combination of all three inhibitors (M, P and A). Statistical analysis was performed on raw data, with asterisks indicating significant inhibitory effect [(*) $p < 0.05$, (**) $p < 0.001$] when compared to the control (**10**).

The combination of MK-801, amantadine and NGP1-01 resulted in slight increase in displacement of compound **10** (55%) when compared to the separate NMDAR inhibitors, confirming our hypothesis that compound **10** binds to the PCP binding site as well as to other sites on the NMDAR (Figures 6 and 7). Compound **10** was not displaced quantitatively (100%) and this was ascribed to the binding kinetics and equipotence of the compounds. Binding to other cell structures also needs to be excluded in future studies.

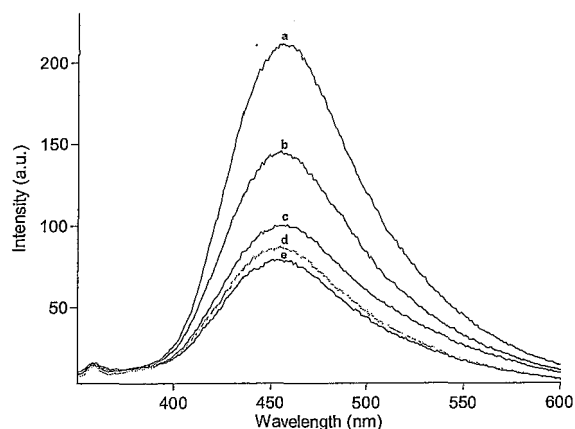


Figure 7: Fluorescent emission spectra of compound **10** (100 μ M) with compound **10** alone (a) (control) and in the presence of (100 μ M) NGP1-01 (b), amantadine (c), MK-801 (d) and (e) consisting of all three NMDAR inhibitors (b, c, and d).

7.5. Conclusion

We described the synthesis, VGCC- and NMDAR-mediated calcium influx inhibition studies, and demonstrated a possible application for this novel group of amantadine and tetradecane polycyclic fluorescent ligands. We have identified fluorescent compounds with long wavelength fluorescence, high Stokes shifts and affinity for the NMDAR and/or VGCC. Further investigations need to be conducted on the displacement of compound **10** as a novel promising ligand for channel research and utilizing the other novel fluorescent NMDAR inhibitors discovered in these studies. Additional fluorescent studies utilizing a fluorescent microscope or confocal laser scanning microscopy could elaborate on the mechanism of action. These compounds could also be used as direct binding calcium channel probes and this will also be investigated for future developments. Ultimately, the use of these ligands might provide an attractive alternative to radioligand binding studies and offer methods to directly study the kinetics of ligand receptor interactions and facilitate in the development of new fluorescent high-throughput assays. Ion channels have become important targets in academic and pharmaceutical research alike. Understanding how ion channels function is critical in determining underlying disease mechanisms and drug interactions. These novel fluorescent polycyclic compounds may also be utilised as multifunctional neuroactive drugs showing NMDAR inhibition, VGCC inhibition, nitric oxide synthase inhibition, antioxidant activity and improved dopamine transmission [25]. Further studies utilizing these structures are underway to establish their usefulness as neuroprotective agents and/or fluorescent ligands to be used in neurodegenerative disorders.

7.6. Experimental

7.6.1. Chemistry: General procedures

Unless otherwise specified, materials were obtained from commercial suppliers and used without further purifications. All reactions were monitored by thin-layer chromatography on 0.20 mm thick aluminium silica gel sheets (Alugram[®] SIL G/UV₂₅₄, Kieselgel 60, Macherey-Nagel, Düren, Germany). Visualisation was achieved using UV light (254 nm and 366 nm), an ethanol solution of ninhydrin or iodine vapours, with mobile phases prepared on a volume-to-volume basis. Chromatographic purifications were performed on silica gel (0.063–0.2mm, Merck) except when otherwise stated. IR spectra were recorded on a Perkin Elmer Spectrum 400 spectrometer, fitted with a diamond attenuated total reflectance (ATR) attachment. Melting points were determined using a Stuart SMP-300 melting point apparatus and capillary tubes. The melting points are uncorrected. High resolution electro spray ionisation (HR-ESI) mass spectra were recorded on a Waters API Q-ToF Ultima mass spectrometer at 70 eV and 100°C. All HR-ESI samples were introduced by a heated probe and perfluorokerosene was used as reference standard. ¹H and ¹³C NMR spectra for all novel compounds were obtained using a Varian Gemini 200 spectrometer at a frequency of 200 MHz and 50 MHz, respectively. All chemical shifts are reported in parts per million (ppm) relative to the signal from TMS ($\delta = 0$) added to an appropriate deuterated solvent. The following abbreviations are used to describe the multiplicity of the respective signals: s – singlet, bs – broad singlet, d – doublet, dd – doublet of doublets, t – triplet, q – quartet and m – multiplet. Compounds **1**, **3**, **5**, **7**, **9**, **11**, **13** and **14** were synthesised and characterised as published in previous publications [24,25] and only the structural data of these derivatives are presented in this paper. The well-described Cookson's diketone, pentacyclo[5.4.0.0^{2,6}.0^{3,10}.0^{5,9}]undecane-8,11-dione (**d**), was synthesised according to the published methods [26,27]. A Cary Eclipse[®] fluorescence spectrometer was used for fluorescence measurements. The fluorescent compounds were measured at a concentration of 10⁻⁵ M in DMSO at room temperature. Emission spectra were recorded at the excitation maximal wavelength.

7.6.1.1. 3-(1-Adamantylamino)propionitrile (b): Adamantane.HCl was converted into the free base by washing it with a water solution saturated with NaHCO₃ to afford the amantadine free base. To a solution of 10 g of amantadine free base in 100 ml of acrylonitrile, 1 ml of H₂O was added and the mixture was heated overnight under reflux. The excess acrylonitrile was removed *in vacuo* and the mixture was added to 100 ml DCM and extracted with brine

(3 x 100 ml), dried over MgSO₄, filtered and concentrated *in vacuo* to give 12.3 g of 3-(1-adamantylamino)propionitrile as a glassy solid (12.3 g, 60 mmol, 91%). **Physical data:** C₁₃H₂₀N₂; **mp:** 48 °C; ¹H NMR (200 MHz, CDCl₃) δ_H: 3.00-2.87 (t, *J* = 6.6 Hz, 2H), 2.51-2.45 (t, *J* = 6.6 Hz, 2H), 2.075 (s, 3H), 1.65 1.61 (m, 12H); ¹³C NMR (50 MHz, CDCl₃) δ_C: 118.96, 51.03, 42.83, 36.81, 36.59, 29.61, 20.21; **IR (ATR; cm⁻¹):** 3307, 2899, 2846, 2246, 1153, 771 cm⁻¹; **HR-ESI⁺:** calcd. 205.1700, exp. 205.1705.

7.6.1.2. *N*-(1-Adamantyl)-1,3-propanediamine (c): To a well-cooled suspension of 3.8 g of LiAlH in 200 ml of dry Et₂O, a solution of 12.3 g in 10 ml Et₂O of 3-(1-adamantylamino)propionitrile (b) was added dropwise. After this addition, the reaction mixture was stirred at room temp for 3 hours. With cooling, 4 ml of H₂O was added, followed by 3 ml 5 *N* NaOH solution, and a further 14 ml of H₂O. The Et₂O layer was decanted, and the solid cake was washed with several portions (5 x 50 ml) of Et₂O. The Et₂O layers were combined, filtered, dried with MgSO₄ and evaporated *in vacuo*, to yield *N*-(1-adamantyl)-1,3-propanediamine as a white wax (10.2 g, 48.97 mmol, 82%). **Physical data:** C₁₃H₂₄N₂; **mp:** wax; ¹H NMR (200 MHz, MeOD) δ_H: 3.22-3.16 (t, *J* = 6.2 Hz, 2H), 2.97-2.91 (t, *J* = 6.1 Hz, 2H), 2.71-2.60 (m, 2H), 2.17-2.10 (m, 3H), 1.91 (bs, 3H) 1.81-1.64 (m, 12H); ¹³C NMR (50 MHz, MeOD) δ_C: 42.63, 41.25, 40.38, 39.92, 38.56, 38.09, 37.78, 37.46, 32.59, 31.60, 31.55, 31.29, 30.29; **IR (ATR; cm⁻¹):** 3360, 2906, 2848, 1550, 1475, 1313, 813, 792 cm⁻¹; **HR-ESI [M+H]⁺:** calcd. 209.2012, exp. 209.2018.

7.6.1.3. 3-Hydroxy-4-aza-8-oxoheptacyclo[9.4.1.0^{2,10}.0^{3,14}.0^{4,9}.0^{9,13}.0^{12,15}]tetradecane (e) [24,28]: **Physical data:** C₁₄H₁₇NO₂; **mp:** 170-172°C; ¹H NMR (300 MHz, CDCl₃) δ_H: 4.97-3.94 (bs, 1H), 3.85-3.74 (m, 2H), 3.73-3.67 (m, 2H), 3.02-2.53 (m, 8H), 1.80:1.52 (AB-q, 2H, *J* = 10.58 Hz), 1.75-1.55 (m, 2H). ¹³C NMR (75 MHz, CDCl₃) δ_C: 101.45, 62.69, 54.97, 53.14, 45.73, 44.63, 44.00, 42.92, 42.41, 41.67, 41.48, 41.01, 24.33; **IR (KBr; cm⁻¹):** 3446, 1484, 1346, 1320, 1166 cm⁻¹; **MS (EI, 70 eV) *m/z*:** 231 (M⁺).

7.6.1.4. *N*-Adamantan-1-yl-2(methylamino)-benzamide (1) [24]: **Physical data:** C₁₈H₂₄N₂O; **mp:** 213°C; ¹H NMR (200 MHz, CDCl₃) δ_H: 8.01-7.97 (dd, *J* = 6.5 and 2.2 Hz, 1H), 7.28 (m, 2H), 6.56-6.62 (m, 3H), 2.86 (s, 3H), 2.00 (s, 3H), 1.86 (d, 6H), 1.62-1.44 (m, 6H); ¹³C NMR (50 MHz, CDCl₃) δ_C: 175.01, 151.75, 132.74, 132.49, 117.54, 113.96, 110.05, 51.09, 40.98, 35.80, 29.74, 29.12; **IR (ATR, cm⁻¹):** 3341, 2911, 2853, 1609; 1503, 1365, 754 cm⁻¹; **HR-ESI [M+H]⁺:** calcd. 284.1888, exp. 284.1886.

7.6.1.5. N-[3-(1-Adamantylamino)propyl]-2-methylamino-benzamide (2): To a solution of *N*-methylantranilic acid (0.28 g, 1.85 mmol) in DMF (10 ml) was added *N,N*-carbonyldiimidazole (0.33 g, 2.035 mmol). The resulting solution was protected from light and warmed at 60 °C for 1 hour and then cooled to room temperature before adding *N*-(1-adamantyl)-1,3-propanediamine (0.383 g, 1.85 mmol). The resulting solution was protected from light and reacted for 48 hours at room temperature and for 6 hour at 60°C to ensure complete reaction. The reaction mixture was added to DCM and extracted with water acidified to pH 3 (3 x 25 ml). The water phase was collected, basified with 5 *N* NaOH (pH 12) and extracted with DCM (3 x 25 mL). The combined organic phases were collected, dried over MgSO₄ and the solvent removed *in vacuo* rendering the crude product as a light yellow oil. The oil was dissolved in ethyl acetate and *N*-hexane was added dropwise until the solution became murky. The mixture was then cooled down to 5°C for crystallization to proceed. The crystals were washed with cold ethyl acetate (2 x 15 ml), yielding the pure product as a light yellow crystalline solid (0.231 g, 0.68 mmol, 37%). **Physical data:** C₂₁H₃₁N₃O; **mp:** 99 °C; **¹H NMR** (200 MHz, CDCl₃) δ_H: 8.58 (bs, NH), 7.76 (bs, NH), 7.46-7.42 (dd, 1H, *J* = 7.6 and 1.4 Hz), 7.30-7.26 (dd, 1H, *J* = 7.6 and 1.4 Hz), 6.67-6.60 (dd, 1H, *J* = 8.4 and 1.4 Hz), 6.59-6.52 (m, 1H), 3.51-3.48 (m, 1H), 2.86-2.79 (m, 5H), 2.06 (m, 3H), 1.75-1.60 (m, 16H); **¹³C NMR** (50 MHz, CDCl₃) δ_C: 169.90, 150.60, 132.55, 127.81, 115.30, 114.21, 111.01, 51.16, 42.62, 40.41, 39.88, 36.75, 29.71, 29.60, 28.95; **IR (ATR; cm⁻¹):** 3302, 3275, 3215, 2908, 2846, 1671, 1627, 1579, 1517, 742 cm⁻¹; **HR-ESI [M+H]⁺:** calcd. 342.2540, exp. 342.2545.

7.6.1.6. N-(1-Cyano-2*H*-isoindol-2-yl)adamantan-1-amine (3) [24]: **Physical data:** C₁₉H₂₀N₂; **mp:** 160°C; **¹H NMR** (200 MHz, CDCl₃) δ_H: 7.69-7.64 (m, 2H), 7.51 (s, 1H), 7.26-7.19 (m, 1H), 7.12-7.04 (m, 1H), 2.45 (m, 6H), 2.32 (s, 3H), 1.83 (m, 6H); **¹³C NMR** (50 MHz, CDCl₃) δ_C: 150.64, 133.86, 125.34, 122.74, 122.39, 120.88, 117.83, 166.59, 115.88, 60.43, 43.00, 35.97, 30.03; **IR (ATR, cm⁻¹):** 3140, 2910, 2850, 2189, 1182.37, 783, 752 cm⁻¹; **HR-ESI [M+H]⁺:** calcd. 276.16366, exp. 276.16265.

7.6.1.7. 2-[3-(1-Adamantylamino)propyl]isoindole-1-carbonitrile (4): *N*-(1-Adamantyl)-1,3-propane-diamine (0.688 g, 3.301 mmol) and NaCN (0.162 g, 3.301 mmol) was dissolved in 20 ml methanol/water. To this was added *o*-phthalaldehyde (0.442 g, 3.301 mmol) and the pH was adjusted to 8-9 with glacial acetic acid. The reaction mixture was protected from light and stirred at room temperature for 24 hours. The mixture was concentrated *in vacuo* and added to an aqueous 1*N* HCl solution and extracted with DCM (3 x 30 ml) and dried over

MgSO₄. The organic fraction was filtered and the solvents removed *in vacuo* yielding a light brown oil. The oil was dissolved in ethyl acetate (25 ml) and cooled down to -15°C while stirring on an external acetone bath. Forced evaporation of the ethyl acetate with a mild stream of N₂ gas caused oversaturation and consequent precipitation of a white solid. The precipitate was filtered and washed with cold cyclohexane yielding the crude product as a white amorphous solid. Purification of the product was accomplished with column chromatography (acetone:ethyl acetate, 3:1) and recrystallization from absolute ethanol rendered the final product as a white microcrystalline solid (0.220 g, 1.223 mmol, 37 %). **Physical data:** C₂₂H₂₉N₃; **mp:** 295 °C; **¹H NMR** (200 MHz, CDCl₃:CD₃OD; 1:1) δ_H: 7.47 (s, 1H), 7.44-7.34 (m, 2H), 7.06-6.90 (m, 1H), 6.91-6.83 (m, 1H), 2.73-2.65 (t, *J* = 7.2 Hz, 2H), 2.13-2.01 (m, 2H), 1.96 (m, 3H), 1.65-1.64 (bs, 6H), 1.54-1.38 (m, 6H); **¹³C NMR** (50 MHz, CDCl₃) δ_C: 131.57, 125.37, 123.95, 122.38, 120.57, 120.22, 117.08, 114.08, 57.21, 47.70, 47.30, 37.80, 36.19, 34.90, 28.58, 27.61; **IR (ATR; cm⁻¹):** 2923, 2852, 2757, 2697, 2488, 2419, 2200, 1689, 1579, 769, 747 cm⁻¹; **HR-ESI [M+H]⁺:** calcd. 334.2282, exp. 334.2283.

7.6.1.8. *N*-Adamantan-1-yl-1*H*-indazole-3-carboxamide (5) [24]: **Physical data:** C₁₈H₂₁N₃O; **mp:** 212°C **¹H NMR** (200 MHz, MeOD) δ_H: 8.26-8.22 (dd, *J* = 6.5 and 2.2 Hz, 1H), 7.54-7.50 (dd, *J* = 6.5 and 2.2 Hz, 1H), 7.38-7.31 (m, 1H), 7.22-7.14 (m, 1H), 2.14 (s, 3H), 1.88 (d, 6H), 1.74-1.72 (m, 6H); **¹³C NMR** (50 MHz, MeOD) δ_C: 170.65, 162.00, 143.29, 127.35, 123.73, 123.66, 122.58, 111.38, 52.64, 47.78, 41.60, 36.51, 30.48; **IR (ATR, cm⁻¹):** 2979, 2909, 2854, 1637, 1475, 1322, 809, 733 cm⁻¹; **HR-ESI [M+H]⁺:** calcd. 295.3886, exp. 295.3669.

7.6.1.9. *N*-[3-(1-Adamantylamino)propyl]-1*H*-indazole-3-carboxamide (6): To a solution of 1*H*-indazole-3-carboxylic acid (0.3 g, 1.85 mmol) in DMF (7 ml) was added *N,N'*-carbonyldiimidazole (0.33 g, 2.035 mmol). The resulting solution was warmed at 60 °C for 2 hours and then cooled to room temperature before adding a solution of *N*-(1-adamantyl)-1,3-propanediamine (0.386 g, 1.85 mmol) in 3 ml DMF. The resulting reaction mixture was stirred for 24 hours at room temperature to completion. After 24 hours the reaction mixture was added to DCM and extracted with water acidified to pH 3 (3 x 25 ml). The water phase was collected and basified with 5 N NaOH (pH 12) and extracted with DCM (3 x 25 mL). The combined organic phases were collected, dried over MgSO₄ and the solvent was removed *in vacuo* rendering the crude product as a yellow oil. The oil was dissolved in ethyl acetate (25 ml) and cooled down to -15 °C while stirring on an

external acetone bath. Forced evaporation of the ethyl acetate with a mild stream of N₂ gas caused oversaturation and consequent precipitation of a white solid. The precipitate was quickly filtered, suspended in water saturated with NaHCO₃, extracted with DCM (3 x 25 ml) and dried over MgSO₄. The solvents were removed *in vacuo* yielding the product as a pale waxy solid. (Yield: 0.288 g, 0.77 mmol, 42 %). **Physical data:** C₂₁H₂₈N₄O; **mp:** wax; **¹H NMR** (200 MHz, MeOD) δ_H: 8.41-8.37 (dd, 1H, *J* = 8.0 and 1.2 Hz), 8.08 (bs, NH), 7.56-7.52 (dd, 1H, *J* = 8.8 and 1.4 Hz), 7.44-7.36 (m, 1H), 7.30-7.23 (m, 1H), 3.60-3.57 (m, 1H), 2.86-2.73 (t, 1H, *J* = 6.6 Hz), 2.067 (m, 3H), 1.92-1.86 (m, 2H), 1.75-1.74 (m, 6H), 1.68-1.56 (m, 6H); **¹³C NMR** (50 MHz, MeOD) δ_C: 163.09, 141.44, 139.64, 127.13, 122.87, 122.63, 122.87, 122.63, 122.25, 109.92, 51.15, 42.61, 38.55, 38.13, 36.81, 30.31, 29.66; **IR (ATR; cm⁻¹):** 3153, 3120, 3063, 2896, 2844, 1670, 1627, 1555, 747 cm⁻¹; **HR-ESI [M+H]⁺:** calcd. 353.2336, exp. 353.2341.

7.6.1.10. *N*-(2,4-Dinitrophenyl)adamantan-1-amine (7) [24]: **Physical data:** C₁₆H₁₉N₃O₄; **mp:** 300 °C; **¹H NMR** (200 MHz, CDCl₃) δ_H: 9.18-9.12 (d, 1H, *J* = 2.2 Hz), 8.81 (s, 1H, NH), 8.23-8.12 (dd, 1H, *J* = 5.1 and 2.2 Hz), 7.25-7.20 (d, 1H, *J* = 5.1 Hz), 2.23 (s, 3H), 2.18-2.08 (m, 6H), 1.82-1.73 (m, 6H); **¹³C NMR** (50 MHz, CDCl₃) δ_C: 147.86, 135.51, 131.02, 129.28, 129.28, 124.97, 116.305, 29.56, 36.15, 42.20, 54.34; **IR (ATR, cm⁻¹):** 3321, 3107, 2927, 2857, 1621, 1587, 1335, 1088, 916, 743 cm⁻¹; **HR-ESI [M+H]⁺:** calcd. 317.13802, exp. 317.13756.

7.6.1.11. *N*-[(3*S*,5*S*,7*S*)-Adamantan-1-yl]-*N'*-(2,4-dinitrophenyl)propane-1,3-diamine (8): 1-Fluoro-2,4-dinitro-benzene (0.354 ml, 1.25 mmol), *N*-(1-adamantyl)-1,3-propanediamine (0.261 g, 1.25 mmol) and K₂CO₃ (0.346 g, 2.5 mmol) was dissolved in 15 ml absolute acetonitrile. The reaction mixture was stirred in the dark for 48 hours, where after the mixture was filtered rendering a yellow precipitate. The precipitate was brought to dryness *in vacuo* and purified by column chromatography (acetone:ethyl acetate, 3:1) yielding the pure product as a yellow amorphous solid (0.411 g, 1.09 mmol, 87 %). **Physical data:** C₁₉H₂₆N₄O₄; **mp:** 168 °C; **¹H NMR** (200 MHz, MeOH) δ_H: 9.04-9.03 (d, *J* = 2.6 Hz, 1H), 8.34-8.28 (dd, *J* = 9.4 and 2.6 Hz, 1H), 7.25-7.21 (d, *J* = 9.4 Hz, 1H), 3.67-3.59 (t, *J* = 7.0 Hz, 2H), 3.11-3.03 (t, *J* = 7.0 Hz, 2H), 2.20 (bs, 3H), 2.11-1.96 (m, 2H), 1.93-1.91 (bs, 6H), 1.86-1.62 (m, 6H); **¹³C NMR** (50 MHz, CDCl₃) δ_C: 149.55, 137.29, 132.04, 131.07, 124.81, 115.71, 57.51, 41.47, 39.91, 38.28, 36.77, 30.65, 27.50; **IR (ATR; cm⁻¹):** 3334, 3111, 2906, 2853, 1616, 1595, 1544, 1520, 1331, 715 cm⁻¹; **HR-ESI [M+H]⁺:** calcd. 375.2027, exp. 375.2032.

7.6.1.12. N-adamantan-1-yl-5-dimethyl-amino-1-naphthalenesulfonic acid (9) [25]:

Physical data: C₂₂H₂₈N₂O₂S; **mp:** 160°C; ¹H NMR (200 MHz, CDCl₃) δ_H: 8.64-8.59 (dd, J = 6.2 and 2.2 Hz, 1H), 8.40-8.36 (dd, J = 6.3 and 2.2 Hz, 1H), 8.28-8.24 (dd, J = 6.3 and 2.1 Hz, 1H), 7.78 (br s, 1H, NH), 7.54-7.40 (m, 2H), 7.13-7.09 (dd, J = 6.4 and 2.1 Hz, 1H), 2.85 (s, 6H, N(CH₃)₂), 1.86 (s, 3H), 1.71 (d, 6H), 1.50-1.28 (m, 6H); ¹³C NMR (50 MHz, CDCl₃) δ_C: 181.38, 140.35, 130.46, 129.92, 127.74, 127.21, 126.34, 123.61, 121.70, 114.69, 52.68, 45.53, 40.12, 35.38, 28.99; **IR (ATR, cm⁻¹):** 3290.86, 2902.11, 2849.28, 2779.45, 1614.28, 1588.52, 1577.02, 1438.47, 1308.27, 1143.95, 1086.98, 783.93 cm⁻¹; **HR-ESI [M+H]⁺:** calcd. 385.1950, exp. 385.1944.

7.6.1.13. N-[3-(1-Adamantylamino)propyl]-5-dimethylaminonaphthalene-1-sulfonamide (10):

N-(1-Adamantyl)-1,3-propanediamine (0.23 g, 1.1 mmol) was dissolved in THF (15 ml) and triethylamine (0.30 g, 2.2 mmol) and cooled on an ice bath. Dansyl chloride (0.30 g, 1.1 mmol) in THF (5 ml) was added and the mixture was stirred for 1h in the ice bath and 24 hours at room temperature. The solvents were removed *in vacuo* rendering a bright yellow oil with a blue luminescence. The yellow oil was added to water acidified to pH 3 (HCl_{aq}) and extracted with DCM (3 x 20 ml), the aqueous layer was collected and made basic with a 10 M NaOH solution to pH 12 and extracted with DCM (3 x 20 ml). The combined organic layers were washed with 10% NaHCO₃ solution (5 x 10 ml) and water (3 x 10 ml), dried with MgSO₄ and concentrated *in vacuo*. The DCM was removed *in vacuo* to render a light yellow oil. The oil was dissolved in acetone and crystals formed on standing. Recrystallization from acetone rendered the desired product as yellowish crystals (0.302 g, 0.68 mmol, 62%).

Physical data: C₂₅H₃₅N₃O₂S; **mp:** 163 °C; ¹H NMR (200 MHz, CDCl₃) δ_H: 8.54-8.49 (d, J = 8.4 Hz, 1H), 8.38-8.34 (d, J = 9.6 Hz, 1H), 8.26-8.22 (dd, J = 7.4 and 1.2 Hz, 1H), 7.58-7.47 (m, 2H), 7.19-7.16 (d, J = 7.4 Hz, 1H), 3.09-3.01 (t, J = 5.6 Hz, 2H), 2.61-2.56 (t, J = 5.6 Hz, 2H), 2.03 (bs, 3H), 1.70-1.54 (m, 6H), 1.53-1.51 (bs, 6H), 1.48-1.40 (m, 2H); ¹³C NMR (50 MHz, CDCl₃) δ_C: 152.00, 135.47, 130.05, 130.03, 129.84, 120.47, 128.19, 123.29, 119.53, 115.12, 50.90, 45.52, 44.36, 42.51, 40.10, 38.72, 29.59, 28.63; **IR (ATR; cm⁻¹):** 3282, 2904, 2847, 2782, 1614, 1589, 1321, 1141, 791 cm⁻¹; **HR-ESI [M+H]⁺:** calcd. 442.2523, exp. 442.2528.

7.6.1.14. N-(1-adamantyl)-2-oxo-chromene-3-carboxamide (11) [25]:

Physical data: C₂₀H₂₁NO₃; **mp:** 300°C; ¹H NMR (600 MHz, CDCl₃) δ_H: 8.90 (s, 1H), 7.71-7.62 (m, 2H), 7.41-7.33 (m, 2H), 2.05 (s, 3H), 1.75-1.64 (m, 12H); ¹³C NMR (150 MHz, CDCl₃) δ_C:

161.60, 159.89, 154.30, 147.64, 133.69, 129.64, 125.13, 119.53, 118.72, 116.48, 52.28, 41.35, 36.34, 30.88, 29.39; **IR (ATR, cm⁻¹):** 3341, 2911, 2853, 1609, 1503, 1365, 754 cm⁻¹; **HR-ESI [M+H]⁺:** calcd. 323.1515, exp. 323.1521.

7.6.1.15. N-(1-Adamantyl)-2-oxo-chromene-3-carboxamide (12): To a solution of coumarin carboxylic acid (0.352 g, 1.85 mmol) in DMF (7 ml) was added *N,N'*-carbonyldiimidazole (0.33 g, 2.035 mmol) in one portion. The resulting solution was stirred at 60°C for 2 hours, where after a solution of *N*-(1-adamantyl)-1,3-propanediamine (0.386 g, 1.85 mmol), in DMF (3 ml) and was added. The resulting solution was reacted for 72 hours at room temperature. It was quenched with a saturated solution of NaCl_(aq) (50 ml). The compound was extracted with ethyl acetate (3 x 30 ml). The combined organic layers were successively washed with 4% citric acid (30 ml), water (30 ml), 4% NaHCO₃ solution (30 ml), and water (30 ml). The organic layer was dried over anhydrous MgSO₄, and the solvent was removed *in vacuo* to provide the crude product as a white crystalline solid. The product was purified by recrystallization from ethyl acetate/petroleum ether (1:1) to afford a white crystalline solid (0.332 g, 0.87 mmol, 47%). **Physical data:** C₂₈H₂₈N₂O₃; **mp:** 211 °C **¹H NMR** (200 MHz, MeOD) δ_H: 8.96 (bs, NH), 8.90 (s, 1H), 7.71-7.62 (m, 2H), 7.42-7.34 (m, 2H), 3.56-3.50 (t, *J* = 6.8 Hz, 2H), 2.79-2.66 (t, *J* = 6.8 Hz, 2H), 2.06 (s, 3H), 1.82-1.74 (m, 1H), 1.74-1.64 (m, 12H); **¹³C NMR** (50 MHz, MeOD) δ_C: 161.70, 161.40, 154.53, 148.25, 134.05, 128.86, 125.33, 118.79, 118.69, 116.72, 50.93, 42.64, 38.26, 38.01, 36.82, 30.72, 29.68; **IR (ATR; cm⁻¹):** 3292, 2902, 2885, 1724, 1709, 1641, 1607, 1568, 759 cm⁻¹; **HR-ESI [M+H]⁺:** calcd. 381.2173, exp. 381.2178.

7.6.1.16. 3-{4-Aza-8-oxo-heptacyclo[0.4.1.0^{2,10}.0^{3,14}.0^{4,9}.0^{9,13}.0^{12,15}]tetradecyl}-2-(methylamino)-benzoate (13) [24]: **Physical data:** C₂₂H₂₁N₃O₃; **mp:** 213°C; **¹H NMR** (300 MHz, CDCl₃) δ_H: 8.14-8.11 (dd, 2H, *J* = 8.19, 0.89 Hz), 7.70-7.67 (dd, 2H, *J* = 8.38, 0.94 Hz), 7.42-7.36 (m, 3H), 7.26-7.21 (m, 3H) 3.89-3.09 (m, 4H), 2.95-2.62 (m, 8H), 2.89-2.87 (d, 2H), 1.89-1.12 (m, 4H). **¹³C NMR** (75 MHz, CDCl₃) δ_C: 166.60, 152.23, 134.75, 131.93, 114.29, 110.68, 109.74, 63.05, 55.52, 43.93, 43.91, 43.88, 29.46, 24.00; **IR (KBr, cm⁻¹):** 3377, 2957, 2360, 1687, 1520, 1343, 1226, 1180 cm⁻¹; **MS (EI, 70 eV) *m/z*:** 364 (M⁺).

7.6.1.17. 3-{4-Aza-8-oxo-heptacyclo[0.4.1.0^{2,10}.0^{3,14}.0^{4,9}.0^{9,13}.0^{12,15}]tetradecyl}-1*H*-indazole-3-carboxylate (14) [24]: **Physical data:** C₂₂H₂₄N₂O₂; **mp:** 190°C; **¹H NMR** (300 MHz, CDCl₃) δ_H: 7.91-7.90 (dd, 2H, *J* = 9.58, 1.14 Hz), 7.38-7.24 (m, 3H), 6.64-6.61 (dd, 2H, *J* = 8.27, 0.79 Hz), 6.57-6.51 (m, 3H), 3.89-3.094 (m, 4 H), 2.95 -2.62 (m, 8H), 2.89 -2.87

(d, 2H, J = 5.99 Hz), 1.81 – 1.50 (m, 4H). ^{13}C NMR (75 MHz, CDCl_3) δ_{C} : 163.47, 140.97, 139.37, 127.06, 123.93, 122.64, 121.66, 110.74, 56.14, 49.96, 49.12, 49.12, 33.89, 30.94, 24.90; IR (KBr, cm^{-1}): 3277, 2931, 2851, 2360, 1625, 1448, 1242 cm^{-1} ; MS (EI, 70 eV) m/z : 375 (M^+).

7.7. Biological evaluation

7.7.1. Imaging experiments using Mag-fura-2AM

7.7.1.1. Materials

All chemicals were of analytical grade or spectroscopy grade and were purchased from Sigma–Aldrich (UK) and Merck (St. Louis, MO, USA).

7.7.1.2. Animals

The study protocol was approved by the Ethics Committee for Research on Experimental Animals of the North-West University (Potchefstroom Campus). Male Sprague–Dawley rats were sacrificed by decapitation and the brain tissue was removed and kept on ice for homogenation. After homogenation, the aliquoted brain homogenate was used immediately or stored at -4°C and used within two days.

7.7.1.3. General Methods

The fluorescent ratiometric indicator, Mag-Fura-2/AM, and a Cary-Eclipse[®] fluorescence spectrometer were used to evaluate the influence of the test compounds on calcium homeostasis *via* the NMDA receptor channel utilizing murine synaptoneuroosomes. Procedures similar to those of published studies were used to prepare the synaptoneuroosomes and solutions, and to establish the techniques for experimental measurement of fluorescence [29]. All data analysis, calculation and graphs were done using Prism 4.02[®] (GraphPhad, Sorrento Valley, CA). Data in bar charts are presented as % values of initial fluorescence with each bar representing the mean \pm SEM. Data analysis was carried out using the Student Newman Keuls multiple range test. Concentration-curve data were analyzed by non-linear least squares fit to a four parameter logistic equation using Prism 4.02[®] (GraphPhad, Sorrento Valley, CA). The level of significance was accepted at $p < 0.05$.

7.7.1.4. Preparation of Synaptoneurosomes

Male adult Sprague-Dawley rats were sacrificed by decapitation, whole brains were removed and synaptoneurosomes were prepared by techniques of Hollingsworth *et al*, slightly modified [35]. The brains from two rats were homogenized (4 strokes by hand using a homogenizer) in 30 ml of ice-cold Krebs-bicarbonate buffer (NaCl, 118 mM; KCl, 4.7 mM; MgCl, 1.18 mM; CaCl₂ 1.2 mM; NaHCO₃ 24.9 mM; KH₂PO₄ 1.2 mM; and glucose, 10 mM). From this step forward the homogenate was kept ice-cold at all times to minimize proteolysis throughout the isolation procedure. The tissue suspension was placed in a 50 ml polycarbonate tube and centrifuged for 15 min at 1100 x g and 0°C. After centrifugation, the pellet was resuspended by hand in 30 ml fresh incubation buffer and centrifuged again as described above. The pellet was gently resuspended in Krebs-bicarbonate buffer at a protein concentration of 3 mg/ml [36]. Protein yield was 10 mg/g tissue.

7.7.1.5 General procedure for loading FURA-2AM and incubating test compounds

Experiments were carried out at 37°C and fluorescence was measured with a spectrofluorimeter equipped with a waterjacketed cuvette holder. The synaptoneurosome suspension prepared was allowed to reach room temperature, thereafter Fura-2 AM (5 mM in DMSO – protect solution from light) was added to a final concentration of 5 µM. Synaptoneurosomes were incubated at 37°C for 10 min, diluted with Krebs-bicarbonate buffer at room temperature to a final concentration of 0.6 mg/ml and kept at room temperature and protected from light until used. Immediately before the experiment, 0.25 ml of the Fura-2 AM synaptoneurosomal suspension was centrifuged for 10 sec in a desk Hermle Z 100 M[®] Microfuge. The supernatant was discarded and the pellet resuspended in 0.75 ml of 37°C Krebs-HEPES buffer (20 mM HEPES substituting for NaHCO₃ and adjusted with NaOH to pH 7.4). For the screening test 100 µM stock solutions of the references and test compounds were prepared in DMSO (final DMSO concentration of 0.1%). 0.75 µl of the stock solution was diluted in 0.75 ml Krebs-HEPES buffer solution to obtain a 100 µM concentration of the test compounds. Control experiments received 0.1% DMSO to compensate for possible effects caused by addition of DMSO in experiments. For the dose response curve, the test compound selected from the screening test was incubated at different concentrations, in a log-scale.

7.7.1.6 KCl mediated calcium stimulation

The wavelengths selected for the detection of intracellular calcium utilizing Fura-2 AM were 344 nm (excitation) and 506 nm (emission) as described in the experimental protocols of previous papers [29]. The optics position was set at the bottom and sensitivity set at 100 with a runtime of 40 seconds with 150 msec intervals. The test compounds were incubated with the synaptoneurosomes for 5 min at 37°C and used immediately after incubation. The procedure was initiated and kept at 37°C. At 10 sec into the recording 100 µl of KCl (140 mM) depolarization solution (43 mM NaCl, 140 mM KCl, 10 mM NaHCO₃, 1.4 mM CaCl₂, 0.9 mM MgSO₄, 5.5 mM Glucose, and 20 mM HEPES, pH 7.4) was added to the membrane preparation to depolarize the synaptoneurosomes and activate calcium influx. Taking the KCl-induced increase in fluorescence as 100%, the percentage that each test compound inhibits the calcium flux, subsequently reducing the fluorescence, can be compared to the reference compounds. To gain a more accurate interpretation of the results, the initial average fluorescence values before application of high concentration potassium (base line) were subtracted from the maximum increase in fluorescence for representative experiments in synaptoneurosomes incubated with test compounds, reference compounds and controls. Standard errors of mean (SEM) values were incorporated as error bars (Figure. 3). Treatments were repeated three times on different tissue preparations with three determinations in each replicate. All the test compounds significantly decreased the KCl mediated calcium flux ($p < 0.05$).

7.7.1.7 NMDA/glycine mediated calcium stimulation

The wavelengths selected for the detection of intracellular calcium utilizing Fura-2 AM were 344 nm (excitation) and 506 nm (emission) as described earlier [29]. The optics position was set at the bottom and sensitivity set at 100 with a runtime of 40 seconds with 150 msec intervals. The test compound was incubated for 5 min at 37°C and used immediately after incubation. Synaptoneurosomes were incubated with the respective compound and because these novel compounds showed VGCC flux inhibition it was co-incubated with the selective voltage gated calcium channel inhibitor, nimodipine (10 µM), to block VGCC thus preventing calcium flux through this channel and allowing selective evaluation of the compounds for the NMDAR. The procedure was initiated and kept at 37°C, at 10 sec into the recording 100 µl of krebs-HEPES buffer containing NMDA (100 µM) and glycine (100 µM) was added to the membrane preparation to stimulate calcium influx through the NMDAR channels. The

addition of NMDA (100 μ M) and glycine (100 μ M) resulted in activation of the NMDAR mediated calcium flux. Treatments were repeated three times on different tissue preparations with three determinations in each replicate.

7.7.1.8 NMDAR competition assay utilizing *N*-[3-(1-adamantylamino)propyl]-5-dimethylamino-naphthalene-1-sulfonamide (10**)**

Murine synaptoneurosomes were prepared as described in 7.1.4. Experiments were carried out at 37°C on a spectrofluorimeter. The synaptoneurosome suspension was allowed to reach room temperature and diluted with Krebs-bicarbonate buffer at room temperature to a final concentration of 0.6 mg/ml. Immediately before the experiment, 0.5 ml of the synaptoneurosomal suspension was centrifuged for 10 sec in a desk Hermle Z 100 M[®] Microfuge. The supernatant was discarded and the pellet was resuspended in 1.5 ml of 37°C Krebs-HEPES buffer. Compound **10** as control (100%) and compound **10** with test derivative(s) were dissolved in DMSO and applied to the synaptoneurosomal preparation at a final concentration of 100 μ M for **10** and the individual test derivatives (final DMSO concentration was kept lower than 0.1%). The reaction was initiated by the addition of 100 μ l Krebs-HEPES buffer containing NMDA (100 μ M) and glycine (100 μ M) to the synaptoneurosomal preparation and incubated for 30 minutes at 37 °C. After 30 minutes the synaptoneurosomal suspension was centrifuged for 10 sec in a desk Hermle Z 100 M[®] Microfuge and the supernatant discarded. At the high test concentration of compound **10** the fluorescent intensities could not be measured before washing of the synaptoneurosomal pellet because of extremely high measurements. The pellet was resuspended in incubation buffer (1.5 ml) and measured spectrofluorometrically at the excitation and emission values of compound **10** (324/455 nm) as there was no spectral shift observed. Compound **10** was used as the control with 100% fluorescent intensity and the decrease in fluorescence caused by the known NMDAR inhibitors were an indication of displacement of compound **10**. All the known NMDAR antagonists did to some degree compete with compound **10** (Figure 6 and 7) for binding with the NMDAR.

7.8. Statistical analysis

All data analysis, calculation and graphs were done using Prism 4.02[®] (GraphPad, Sorrento Valley, CA). Data in bar charts are presented as % values of initial fluorescence with each bar representing the mean \pm SEM. Concentration-curve data was analyzed by non-linear least

squares fit to a four parameter logistic equation using Prism 4.02[®]. Data analysis was carried out using the Student Newman Keuls multiple range test of test compounds versus controls in the screening studies. The level of significance was accepted at $p < 0.05$. Bonferroni's Multiple Comparison, one way analysis of variance (ANOVA) was performed on selected data to indicate significant differences between test compounds ($p < 0.05$ was considered to be a statistically significant difference).

Acknowledgments

We are grateful to the North-West University, University of the Western Cape, Medicine Research Council of South Africa and the National Research Foundation of South Africa for financial support.

Supplementary data

¹H-NMR and ¹³C-NMR spectra for all synthesised compounds are presented in Annexure E

References

- [1] H.P. Rang, M.M. Dale, J.M. Ritter, Rang and Dale's Pharmacology, Elsevier, Philadelphia, 2007, chap.35, pp. 508.
- [2] T. Araki, T. Kumagai, K. Tanaka, M. Matsubara, H. Kato, Y. Itoyama, Y. Imai, Brain res. 918 (2001) 176-181.
- [3] T. Alexi, C.V. Borlongan, R.L.M. Faull, C.E. Williams, R.G. Clark, P.D. Gluckman, P.E. Huges, Prog Neurobiol. 60 (2000) 409-470. (b) J.G. Greene, J.T. Greenamyre, Prog Neurobiol. 48 (1996) 613-634.
- [4] J.A. Kemp, R.M. McKernan, Nat Neurosci. 5 (2002) 1039-1042.
- [5] M.F. Cano-Abad, M. Villarroya, A.G. García, N.H. Gabilan, G. Manuela, M.G. López, J Biol Chem. 276 (2001) 39695-39704.
- [6] D.W. Choi, Neurosci Lett. 58 (1985) 293-297. (b) G. Garthwaite, F. Hajos, J. Garthwaite, Neuroscience. 18 (1985) 437-447. (c) R.P. Simon, T. Griffiths, M.C. Evans, J.H. Swan, B.S. Meldrum, J Cereb Blood. Flow. Metab. 4 (1984) 350-361. (d) R.P. Simon, J.H. Swan, B.S. Meldrum, Science. 244 (1984) 798-800.

- [7] M. Arundine, M. Tymianski, *Cell Mol Life Sci.* 61 (2004) 657-668.
- [8] W.J. Geldenhuys, S.F. Malan, J.R. Bloomquist, A.P. Marchand, C.J. Van der Schyf, *Med Res Rev.* 25 (2005) 21-48. (b) W.J. Geldenhuys, S.F. Malan, T. Murugesan, C.J. Van Der Schyf, *Bioorg Med Chem.* 12 (2004), 1799-1806.
- [9] C.G. Parsons, W. Danysz, G. Quack, *Neuropharm.* 38 (1999) 735-767.
- [10] H.V. Chen, S.A. Lipton, *J Neurochem.* 97 (2006) 1611-1626.
- [11] C.J. Van der Schyf, G.J. Squier, W.A. Coetzee, *Pharmacol Res Commun.* 18 (1986) 407-417.
- [12] W.J. Geldenhuys, S.F. Malan, J.R. Bloomquist, C.J. Van der Schyf, *Bioorg Med Chem.* 5 (2007) 1525-1532.
- [13] C. Kiewert, J. Hartmann, J. Stoll, T.J. Thekkumkara, C.J. Van der Schyf, J. Klein, *Neurochem Res.* 31 (2006) 395-399.
- [14] A. Mdzinarishvili, W.J. Geldenhuys, T.J. Abbruscato, U. Bickel, J. Klein, C.J. Van der Schyf, *Neurosci Lett.* 383 (2005) 49-53.
- [15] W.J. Geldenhuys, S.F. Malan, T. Murugesan, C.J. Van der Schyf, J.R. Bloomquist, *Bioorg Med Chem.* 12 (2004) 1799-1806.
- [16] W.J. Geldenhuys, G. Terre'Blanche, C.J. Van der Schyf, S.F. Malan, *Eur J Pharmacol.* 458 (2003) 73-79.
- [17] R.T. McCabe, D.R. Mahan, R.B. Smith, J.K. Wamsley, *Pharmacol Biochem Behav.* 37 (1990) 365-370. (b) C.J. Daly, J.C. McGrath, *Pharmacol Therapeut.* 100 (2003) 101-118.
- [18] M. Auer, K.J. Moore, F.J. Myers-Almes, R. Guenther, A.J. Pope, K.A. Stoekli, *Drug Discov Today.* 3 (1998) 457-465. (b) J.C. McGrath, S. Arribas, C.J. Daily, *Trends Pharmacol Sci.* 17 (1996) 393-399. (c) R.T. McCabe, A.H. Newman, P. Skolnick, *J Pharmacol Exp Ther.* 262 (1992) 734-740.
- [19] M. Leopoldo, E. Lacivita, F. Berardi, R. Perrone, *Drug Discov Today.* 14 (2009) 709-712.

- [20] S.F. Malan, A. Van Marle, W.M. Menge, V. Zuliana, M. Hoffman, H. Timmerman, R. Leurs, *Bioorg Med Chem.* 12 (2004) 6495-6503.
- [21] R.J. Middleton, B. Kellam, *Curr Opin Chem Biol.* 9 (2005) 517-525.
- [22] C. Hödl, W.S.L. Strauss, R. Sailer, C. Seger, R. Steiner, E. Haslinger, H.W. Schramm, *Bioconjugate Chem.* 15 (2004) 359-365. (b) S.X. Xie, G. Petrache, E. Schneider, Q.Z. Ye, G. Bernhardt, R. Seifert, A. Buschauer, *Bioorg Med Chem Lett.* 16 (2006) 3886-3890. (c) M. Cowart, G.A. Gfesser, K. Bhatia, R. Esser, M. Sun, T.R. Miller, K. Krueger, D. Witte, T.A. Esbenshade, A.A. Hancock, *Inflamm. Res.* 55 (2006) S47-S48. (d) R.J. Middleton, S.J. Briddon, Y. Cordeaux, A.S. Yates, C.L. Dale, M.W. George, J.G. Baker, S.J. Hill, B. Kellam, *J Med Chem.* 50 (2007) 782-793. (e) M. Amon, X. Ligneau, J.C. Camelin, I. Berrebi-Bertrand, J.C. Schwartz, H. Stark, *ChemMedChem.* 2 (2007) 708-716. (f) E. Schneider, M. Keller, A. Brennauer, B.K. Hoefelschweiger, D. Gross, O.S. Wolfbeis, G. Bernhardt, A. Buschauer, *ChemBioChem.* 8 (2007) 1981-1988; (g) D.H. Singleton, H. Boyd, J.V. Steidl-Nichols, M. Deacon, M.J. de Groot, D. Price, D.O. Nettleton, N.K. Wallace, M.D. Troutman, C. Williams, J.G. Boyd, *J Med Chem.* 50 (2007) 2931-2941. (h) L.H. Jones, A. Randall, C. Napier, M. Trevethick, S. Sreckovic, J. Watson, *Bioorg Med Chem Lett.* 18 (2008) 825-827.
- [23] M. Deacon, D. Singleton, N. Szalkai, R. Pasieczny, C. Peacock, D. Price, J. Boyd, H. Boyd, J. Steidl-Nichols, C.J. Williams, *Pharmacol Toxicol Methods.* 55 (2007) 255-264.
- [24] J. Joubert, S. Van Dyk, S.F. Malan, *Bioorg Med Chem.* 16 (2008) 8952-8958.
- [25] J. Joubert, S. Van Dyk, I.R. Green, S.F. Malan, *Bioorg Med Chem.* 19 (2011) 3935-3944.
- [26] R.C. Cookson, E. Grundwell, R.R. Hill, J. Hudec, *J Chem Soc.* (1964) 3062-3075.
- [27] R.C. Cookson, E. Grundwell, E., J. Hudec, *Chem Ind.* 39 (1958) 1003-1004.
- [28] L.H.A. Prins, A. De Vries, M.R. Cairns, D.W. Oliver, S. Van Dyk, S.F. Malan, *J Chem Cryst.* 39 (2008) 705-709.
- [29] (a) S.J. Benavide, Y. Claustre, B. Scatton, *J Neurosci.* 10 (1988) 3607-3615. (b) J.N. Crawley, C.R. Gefen, M.A. Rogawski, D.R. Sibley, P. Skolnick, S. Wray, *Current protocols in neuroscience.* 2001. Retrieved 3 June 2008, from <https://commerce.invitrogen.com>. (c)

W.J. Geldenhuys, S.F. Malan, J. R. Bloomquist, C.J. Van der Schyf, *Bioorg Med Chem.* 15 (2007) 1525-1532. (d) D.G. Lambert, Ed. Calcium signaling protocols. 1999. *Methods in molecular biology*. Totowa, New Jersey, Humana Press. (e) A.K. Stout, I. J. Reynolds, *Neurosci.* 89 (1991) 91-100. (f) A.P. Takahashi, E.A. Camacho, *Physiol Rev.* 74 (1991) 1089-1125.

[30] W. Liebenberg, J.J. Van der Walt, C.J. Van der Schyf, *Pharmazie.* (2000) 833-836

[31] A.L. Sobolevsky, S.G. Koshelev, B.I. Khodorov, *J Physiol.* 512 (1998) 47-60.

[32] S.A. Lipton, Y. Choi, H. Takahashi, D. Zhang, L. Weizhong, A. Godzik, L.A. Bankston. *Trends Neurosci.* 25 (2002) 474-480.

[33] H.J.R. Lemmer, J. Joubert, S. van Dyk, F.H. van der Westhuizen, S.F. Malan, *Med Chem.* In press.

[32] R. Dingleline, K. Borges, D. Bowie, S.F. Tryanellis, *Pharmacol Rev.* 51 (1999) 7-61.

[33] E.B. Hollingsworth, E. T. McNeal, J. L. Burton, R. J. Williams, J. W. Daly, C. R. Creveling. *J Neurosci.* 5 (1985) 2240-2253.

[34] K. Resch, W. Imm, E. Ferber, D.F.H. Wallach, H. Fischer, *Naturwissenschaften.* 58 (1971) 220-221.